Chemical Engineering Journal 501 (2024) 156236

Contents lists available at ScienceDirect

Chemical Engineering Journal

journal homepage: www.elsevier.com/locate/cej

Tetracycline degradation for wastewater treatment based on ozone nanobubbles advanced oxidation processes (AOPs) – Focus on nanobubbles formation, degradation kinetics, mechanism and effects of water composition

Priya Koundle [a], Neelkanth Nirmalkar [a,*], Malwina Momotko [b], Sławomir Makowiec [c], Grzegorz Boczkaj [b,d,*]

[a] Department of Chemical Engineering, Indian Institute of Technology Ropar, Rupnagar 140001, India
[b] Department of Sanitary Engineering, Faculty of Civil and Environment Engineering, Gdansk University of Technology, Gdansk, G. Narutowicza St. 11/12, Poland
[c] Department of Organic Chemistry, Faculty of Chemistry, Gdansk University of Technology, Gdansk, G. Narutowicza St. 11/12, Poland
[d] School of Civil, Environmental, and Architectural Engineering, College of Engineering, Korea University, 145 Anam-ro, Seongbuk-gu, Seoul 02841, Republic of Korea

ARTICLE INFO

Keywords:
Emerging contaminats
Mass transfer coefficient
Radical scavengers
Synergistic coefficient
Wastewater treatment
Water chemistry

ABSTRACT

Presence of pharmaceuticals, especially antibiotics, in industrial and domestic effluents causes serious damage to the environment. Classic wastewater treatment processes, in particular conventional biological treatment methods, are not sufficient to rapidly eliminate antibiotics. Typically, Advanced Oxidation Processes (AOPs) based on activation of hydrogen peroxide, ozone or persulfate for formation of particular type of radical species or singlet oxygen are used. A one of cutting-edge technologies to increase effectiveness of AOPs based on ozone are nanobubbles based processes. Thus, this paper focuses on utilization of ozone in the form of nanobubbles for degradation of tetracycline (TC). The effects of several reaction parameters, such as antibiotic concentration, ozone intake, pH, presence of salts, were investigated. This study revealed that the presence of ozone nanobubbles had a substantial positive impact on the degradation of TC. This improvement may be attributed to the enhanced mass transfer and the production of reactive radicals that occur during the collapse of the nanobubbles. Identification of Reactive Oxygen Species (ROS) revealed a significant contribution of hydroxyl radicals in the degradation of the antibiotic. AOP based on O_3 nanobubbles generated mostly hydroxyl ($^{\bullet}OH$) and superoxide anion ($O_2^{\bullet-}$) radicals providing 100 % degradation of 100 mg/L TC within 20 min at 8 mg/L ozone concentration. Based on identified by LC-MS intermediates a detailed degradation mechanism has been described. Degradation of TC and intermediates transformations included methylation, hydroxylation, ring-opening steps as well as cleavage of C-N bonds. This research introduces a novel technique combining nanobubbles with advanced oxidation processes (AOPs), which is anticipated to provide enhanced efficiency and environmental sustainability.

1. Introduction

The COVID-19 outbreak has had a significant impact on global public health, resulting in nearly 6.5 million fatalities. The World Health Organization has declared the COVID-19 a "public health emergency of international concern" [1,2]. During the early stages of the pandemic, infected individuals displayed symptoms similar to bacterial pneumonia and were incorrectly treated with antibiotics that are ineffective against viral respiratory illnesses [3,4]. High levels of antibiotics in hospital effluent have been linked to the high frequency of antibiotic treatments in medical facilities [5]. Human consumption of antibiotics rose 39 % globally between 2000 and 2015, and it is predicted that by 2030, antibiotic use may reach 200 % of that level [6]. After being administered therapeutically, the majority of them are expelled by people into the sewage system, where wastewater treatments only remove a portion of them. To avoid contamination of receiving waters, the parent chemicals and their metabolites are released [7]. As a result, one of the main factors contributing to antibiotic resistance is the widespread use of

* Corresponding authors.
E-mail addresses: n.nirmalkar@iitrpr.ac.in (N. Nirmalkar), grzegorz.boczkaj@pg.edu.pl (G. Boczkaj).

https://doi.org/10.1016/j.cej.2024.156236
Received 15 May 2024; Received in revised form 24 September 2024; Accepted 26 September 2024
Available online 5 October 2024

antibiotics in a variety of settings, including soil [8], water, and sludge [6]. The emergence and spread of antibiotic resistance genes (ARGs) in the environment have consequently raised concerns about public health, particularly the prevention and management of human illness [9–11]. Antibiotics, a class of medicines, are widely used in treatments and are recognized as a prominent category of persistent pollutants. Their presence in aqueous streams through the discharge of animal husbandry, pharmaceutical wastewater, and medical wastewater raises significant environmental concerns [12–15]. Frequently used pharmaceutical medications include ibuprofen, metformin, tetracycline, and acetylsalicylic acid, among others [16]. Among the antibiotics, tetracycline is one of the broad-spectrum antibiotics, effective against infections caused by gram-positive and negative microorganisms, mycoplasma, and protozoan parasites. It is used extensively in veterinary medicine, human treatment and the agricultural industry as a feed ingredient [17,18]. Tetracycline is often used as a growth promoter in aquaculture to amplify nutrient absorption, hence facilitating farmers in augmenting production and productivity [19]. The persistent use and inadequate handling practices contribute to the identification of tetracycline in various water matrices including surface water, ground water, sewage water, and drinking water, range from nanograms per litre (ng/L) to micrograms per litre (μg/L) [20–22]. In the long term, tetracycline presents a substantial risk to both plant and animal life. Therefore, it is essential to create efficient remediation technology in order to guarantee the elimination of tetracycline from wastewater [23].

Amongst the various techniques, advanced oxidation processes such as Fenton/Fenton-like oxidation [24], photocatalysis [25,26], electrocatalysis [27], ozone oxidation [28,29], ultrasound [30,31] are the best recommended technologies for the treatment of the organic pollutants present in wastewater [32]. The underlying principle of the advanced oxidation process is the generation of reactive oxygen species, including hydroxyl radicals, that help in the degradation of the organics [33,34]. The utilisation of AOPs, specifically ozone-based AOPs, has become prevalent in the oxidation and potential mineralization of diverse harmful and resistant organic pollutants in wastewater, intending to attain sustainable development goals (SDGs) [35]. These processes derive their efficacy from the consistent production of potent hydroxyl radicals ($^{\bullet}$OH) and ROS [36,37]. Although there has been significant progress in the creation of very effective catalysts for catalytic ozonation processes, the stability and deactivation of these catalysts during prolonged operation have severely limited their commercial uses [38,39]. Khan et al. [88] studied the degradation of tetracycline by conventional ozonation and investigated effects of pH variations, protonation and dissociation of functional groups and variation in free radical exposure were investigated to elucidate the transformation pathway. The toxicity of TC was decreased at a faster rate at pH 7.0 than pH 2.2. The removal of TOC reached a maximum of ≈40 % after 2 h of ozonation. O_3-based AOPs procedures for wastewater treatment are further hampered by the limited solubility and low mass transfer of ozone, which result in high operating costs [40,41]. The addition of nanobubble technology to the ozonation process (O_3/NBs) holds a great potential to supplement the current conventional AOPs for efficient pollutant removal because it has a higher ROS generation rate and improved gas mass transfer efficiency than conventional ozonation technology (O_3 macrobubbles) [41,42,92]. Nanobubbles are gas-filled cavities owing to some distinctive properties such as high stability [43], a high surface area to volume ratio [44], high negative zeta potential [45], low buoyancy [46], and the ability to generate radicals [47] which allow them to contribute to physical, chemical and biological water treatment processes in many ways [48]. Yang et al. [55] investigated the oxidative capacity of reactive oxygen species (ROS) produced by ozone bubbles of different sizes. The results showed the generation of ROS because of bubble shrinkage and collapse. Hydroxyl radicals were produced after the reaction between ozone and hydroxide ions. Tetracycline in its various chemical forms has been studied using the micro nanobubble technology for its removal from the wastewater. Wang et al. [49] studied the degradation of oxytetracycline using oxygen nanobubbles coupled with photodegradation. With the rise in pH (4.0–11.0), the photodegradation efficiency of OTC increased from 45 to 98 percent. Quenching tests showed that the photodegradation of OTC was mostly caused by the $^{\bullet}$OH radical as the active species [49]. Chen et al. [50] investigated the effect of activated hydrogen peroxide on the degradation of tetracycline hydrochloride using air micro and nanobubbles. Also, MNBs (micro-nano bubbles) with ozone in wastewater treatment, improved ozone's mass transfer efficiency and boosted ozone solubility and also helped in lengthening the reaction activity. Numerous experimental researches on micro-nano bubbles in combination with other processes have been conducted [51,52,53].

Although there are recent studies on the degradation of the tetracycline using oxygen [49] and air micro and nanobubbles [50], and ozone microbubbles [86]. Wang et al. [86] studied the degradation of TC using ozone microbubbles of size less than 50 μm with 500 mg/L of TC concentrations. It was evident from the rate constants that tetracycline degraded more rapidly in acidic solutions than in basic ones. Radical scavenging and mineralization experiments were also performed. However, little emphasis has been placed on investigating the associated reaction kinetics, degradation routes, and nanobubble generation. Studies available on the degradation of the antibiotic tetracycline using ozone in the form of nanobubbles are scarce and only some preliminary attempts were published. Thus, the major objective of this work is to study the degradation of tetracycline using ozone as a potential oxidant in the form of nanobubbles. Furthermore, various parameters such as ozone flow rates (2.5–10 L/min), initial tetracycline concentration (100–400 mg/L), varying pH (4–11), addition of salts (NaCl, 0.1–100 mM) and scavenging experiments were performed. Radical quenching experiments, reaction kinetics, and liquid chromatography coupled to mass spectrometry (LC-MS) were performed owing to the explanation of the degradation mechanism of tetracycline. This study aimed to develop a catalyst-free and green technology method for the degradation of antibiotics.

2. Materials and methods

2.1. Chemicals and reagents

Tetracycline (98 %) was purchased from Sigma Aldrich and was used without any further purification. Sodium chloride (NaCl, 99.5 %), sodium hydroxide (NaOH, 97 %), hydrochloric acid (HCl, 37 %), 2-Propanol ($(CH_3)_2CHOH$, 99.5 %) and ethanol were purchased from Merck chemicals. Pure water was gathered from the Milli-Q system (Milli-Q Direct-16 water purification system) having a resistivity of 18.2 MΩ·cm^{-1} and pH of 7.1 at a temperature of 25 °C and that has been used in all the experiments. Before the experiment, distilled water and all stock solutions were checked using a NanoSight NS300 (Malvern Instruments, UK) for nanoscale contaminants, however, no appreciable quantities of nanoscale entities were discovered. A stock solution and the experiment water were assessed using NanoSight before the testing to rule out any prior nanoscale contamination. When handling and maintaining the experimental setup, additional safety precautions have been adopted. Disposable pipettes, vials, and syringes devoid of latex were used to avoid contamination.

2.2. Experimental setup

The experimental setup is presented in Fig. 1. The stock solutions for tetracycline (TC) were prepared by adding the desired amount of tetracycline to Milli-Q water in the beaker and stirring it magnetically for 45 min at 600 rpm. For the ozonation to be carried out, the experimental setup consisted of an acrylic tank (10″ × 10″ × 15″ (L × B × H)), a circulating pump (Earth 12 V DC 150 psi Diaphragm Motor Pump Diaphragm Water Pump), an ozone generator (ISM 5-OXY, OZ-Air (India)), an oxygen concentrator, and a nanobubble generator (manufactured by

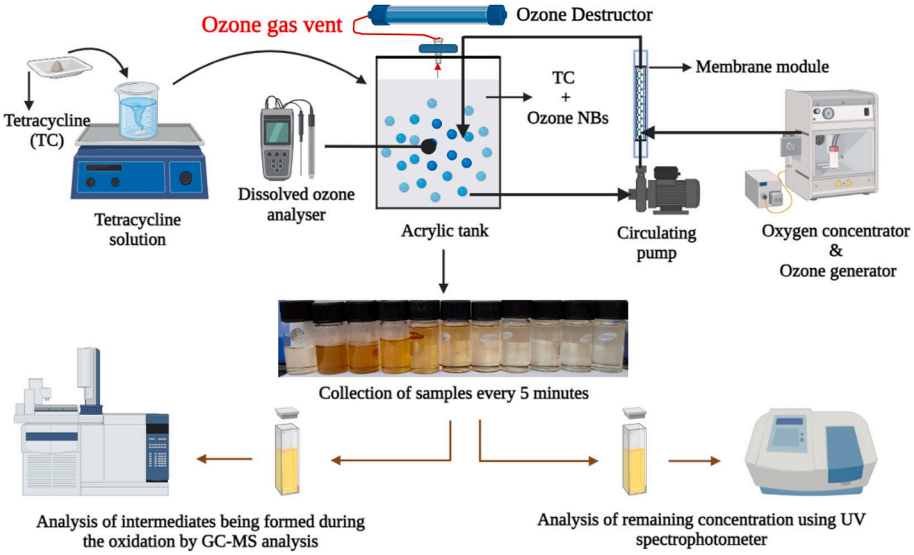

Fig. 1. Illustrative representation of the experimental set-up for the degradation of tetracycline. The dissolved ozone has been measured online using the dissolved ozone analyser. The degradation of TC is characterized by analysis through UV Spectrophotometer and LC-MS analysis. Photography of collected samples document real change of color of treated solution, while treatment.

NanoKriti Pvt. Ltd. India) which were used for the generation of nanobubbles. The ozone was produced through the corona discharge with a purity of 5–8 wt%. A pressure gauge was also installed in the ozone gas sparging line connected to the nanobubble generator. With varying ozone flow rates, the gas sparging pressure measured to be in the range of 40–50 kPa during the experiments.

The ozone nanobubbles were generated using the nanopore diffusion method and varying the ozone flow rates from (2.5 to 10 L/min, 40–50 kPa). The set up was run for a period of 30 min in recirculation mode. Ozone gas was fed from the ozone generator, flow rate of which was controlled through an ozone rotameter (1–10 L/min, Flowstar Engineering Pvt. Ltd). The dissolved ozone was measured online using a dissolved ozone analyser (Q46H, Analytical Technology Inc., Collegeville, Pennsylvania, US). The dissolved ozone monitor used a polarographic membrane sensor to determine the dissolved ozone concentration accurately. The display range of the monitor was 0–200.0 mg/L, and the accuracy was ±0.1 mg/L. Calibrations for the analyser were performed beforehand using Ozone Zero Cal and Ozone Span Cal method. The excess ozone produced during the ozonation experiments were fed to the ozone destructor (OD-10, Ozone Destructor, Faraday Ozone) which was placed above the acrylic tank. The destructor works on a catalytic reaction where MnO_2 worked as a catalyst to convert the excess ozone gas to oxygen before releasing it to the atmosphere. The experiments were performed in a room with air-conditioning. The diaphragm pump used for the recirculation of the solution helped in maintaining the temperature at ambient conditions as the heat losses were minimized. The sample was collected in a glass vial after a period of 30 min and further characterized using NTA analysis (detailed explanation provided in Supporting Information, Fig. SI 7). The experimental protocol to study different parameters is as follows: the prepared stock solution of TC was placed in the acrylic tank and the setup was run in a recirculation mode with ozone being fed to the nanobubble generator from the ozone generator. The experiment was run for 60 min and the samples were collected every five minutes. Various parameters such as ozone flow rates (2.5–10 L/min, 40–50 kPa), initial tetracycline concentration (100–400 mg/L), varying pH (4–11), addition of salts (NaCl, 0.1–100 mM) and scavenging experiments were performed. The removal rate was calculated as follows:

$$\%removal = \frac{(C_{AO} - C_A)}{C_{AO}} \quad (1)$$

For the kinetic studies of TC degradation, after analysis for the correlations of zeroth, first and second order reactions [50], it was clear that the degradation of TC were observed to bear a second order kinetics as follows:

$$-r_a = k\,C_A^2 \quad (2)$$

Upon integrating Eq (2). from t = 0; $C_A = C_{AO}$ to t = t; $C_A = C_A$, we get the following expression as in Eq (3).

$$\frac{1}{C_A} = \frac{1}{C_{AO}} + kt \quad (3)$$

where C_A is the concentration of TC at any time t, C_{AO} is the initial concentration of TC taken, t is the time and k is pseudo second order rate constant.

The volumetric mass transfer coefficient was determined by measuring the dissolved ozone concentration through a dissolved ozone analyzer. The ozone concentration was measured by passing the ozone gas through the membrane module as depicted in Fig. 1 into the liquid tank, where the ozone analyzer was placed for the measurements. The concentration was recorded at every 1-minute interval. The mass balance equation for dissolved ozone can be given as:

$$-\frac{dC}{dt} = k_L a\,(C^* - C_t) - k_d C_t \quad (4)$$

where C* (mg/L), C_t (mg/L), k_d, k_La and C_O (mg/L) are the saturated concentration, concentration at any given time t (min), ozone decomposition rate constant, volumetric mass transfer coefficient of ozone (min^{-1}) and initial concentration (mg/L), respectively. The time t is measured in minutes. At the initial condition of t = 0, the concentration $C_t = C_O$. Integrating Eq.4 for $k_d = 0$ yields the following expression as in Eq.5 [54], which is the case when pure water is being used. The reason for neglecting self-decomposition $k_d = 0$ of ozone is that the entirety of the experiment was conducted while ozone nanobubble generation was taking place inside the reaction vessel. According to the recent literature it is safe to assume that the self-decomposition of the ozone would be insignificant as compared to the accumulation of ozone into the system during the ozone nanobubble generation process [55,56].

$$\ln\left(\frac{C^* - C_t}{C^* - C_O}\right) = (k_L a)t \quad (5)$$

In the present case, when TC is present in the solution, the model equation required to calculate the mass transfer coefficient can be derived from Eq.4. Solving Eq.4 and re-arranging the variables, the final equation is in the form Eq. (6). Finally, the value of k_d will be substituted in Eq.6.

$$\frac{C_t}{C^*} = \frac{k_L a}{k_L a + k_d}\left(1 - e^{-(k_L a + k_d)t}\right) \quad (6)$$

Consequently, the rate constant of the ozone consumed by chemical reaction over time can be measured by the following equation by determining the slope of the curve fit for the data of O_3 concentration versus time curve [55]:

$$\frac{C_t}{C^*} = e^{-k_d t} \quad (7)$$

The sample calculations to estimate the mass transfer coefficient from Eq. (6) have been presented in SI.

2.3. Analytical procedures

A spectrophotometer (DR3900, HACH) was used for the detection of the concentration of TC remaining in the samples after the degradation. The absorbance curves were calculated and attained a maximum value at a wavelength of 357 nm [57]. The calibration curve was plotted at various concentrations of TC (1–50 mg/L, 100–400 mg/L) with R^2 = 0.99 has been presented in supporting information (Fig. SI 6). The radicals generated during the ozonation process were qualitatively measured by radical scavenging experiments. 2-Propanol was used as a radical scavenger for •OH radical as it inhibits the activity of the •OH radicals. The intermediates formed during the process were analyzed by LC-MS. The degradation of TC was analyzed on a LC-MS instrument (XEVO G2-XS QTOF, Waters). An electrospray ionization (ESI) in a positive mode was used with analysis of full scan range from 0 to 1000 with a C18 column (Symmetry C18 Column, 4.6 mm × 250 mm, 3.5 μm). The set up was run with mobile phase of 50:50 % acetonitrile and water [58]. Nanobubbles were characterized using Nanoparticle Tracking Analysis (NS300, Malvern) (detailed explanation provided in Supporting Information, Fig. S7).

3. Results and discussions

3.1. Effect of TC dosage on degradation kinetics

The generation of ozone nanobubbles was performed using nanopore diffusion methods. Ozone nanobubbles were characterized by nanoparticle tracking analysis (NTA), as shown in Fig. 2. The bubble number density shows a positive correlation with the ozone flow rate. Furthermore, to ascertain the contamination, the nanobubble refractive index (RI) was estimated, and the refractive index was close to unity, confirming that the measurement relates to nanobubbles [59]. The stability of ozone nanobubbles was studied over a period of 30 days (results presented in Supporting information Fig. S6). Nanobubbles seem to disappear at a slower rate at high concentration of ozone nanobubbles as in the case of 10 L/min. Even after 30 days, a considerable amount of nanobubbles are still present in the solution. Meanwhile, the mean bubble diameter experiences a relatively small but significant increase from 230 to 260 nm in case of 2.5 L/min of ozone flow rates.

To study the effect of the initial concentration of TC and ozone intake, the experiments were performed at different reaction conditions. The initial concentrations of TC were varied from 100 to 400 mg/L. The flow rates of ozone were taken from the start of 2.5 standard litre per minute (L/min), 5 L/min to the highest of 10 L/min values. The setup was run in a re-circulation mode and ozone was fed to the reactor to produce ozone nanobubbles. The amount of ozone being fed to the reactor plays a major role in the degradation process as it is an important aspect on which the degradation is dependent. The nanobubble characterization at different ozone flow rates was done using NTA (Nanoparticle Tracking Analysis, Malvern). The results of the characterization are depicted in Fig. 2. Based on the obtained results, it can be clearly depicted that at 10 L/min, the highest amount of nanobubbles are being formed with the highest intensity. The results for varying initial concentration of TC and ozone intake are depicted in Fig. 3 where the trends for the decrease in the concentration of TC are shown. From Fig. 3 (i), (ii), and (iii), it can be evaluated that the lower the concentration of the antibiotic, the lesser is the time needed for the quantitative degradation. The initial concentration of 100 mg/L achieves 100 % degradation within 15 min in the case of 10 L/min ozone flow rate. Subsequently at 5 and 2.5 L/min, the time taken is 30 and 35 min respectively. Following this, as the concentration of TC is increased from 100 to 400, the time needed to obtain 100 % degradation also increases. This phenomenon is observed in respect to all studied conditions (ozone flow rate values). The rate constant was calculated for each set of experiments and their values were compared. Fig. 3 (iv), (v) and (vi) show that the reaction kinetics follows the second order reaction with coefficient of determination, $R^2 = 0.98$. It can be clearly noticed, that at 10 L/min the reaction rates were the highest with a value of 0.01285 L $mg^{-1}min^{-1}$ at 100 mg/L of TC. Overall, based on this part of experiments, it can be concluded that the best degradation results were achieved at 10 L/min as the highest rate constants were achieved here. The probable reason for this would be the amount of dissolved ozone present at that particular flow rate. Since ozone is acting as the prime free radical source responsible for the degradation of tetracycline, the amount of ozone being generated during these experiments plays a vital role. The online measurements were done for the dissolved ozone during the degradation process at each initial concentration of TC as well as when no antibiotic was present. Also, the molar ratio (Ozone/TC), degradation efficiency of TC and molar excess of ozone were compared to find out the plausible reason for

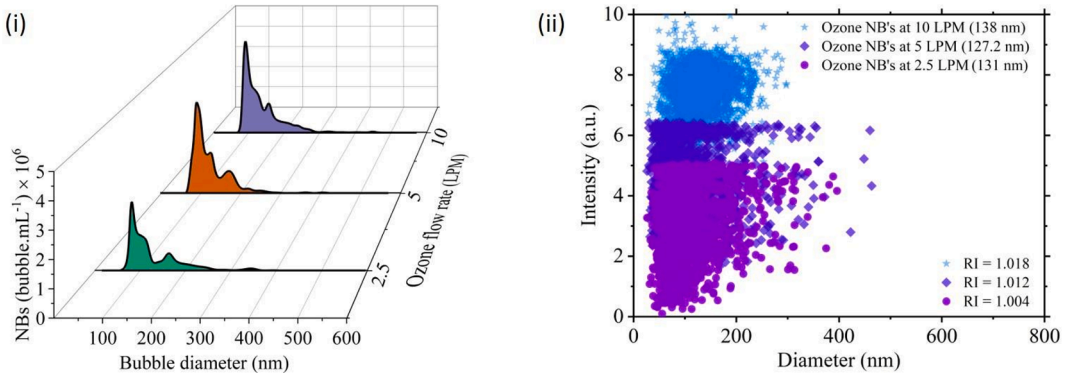

Fig. 2. Effect of ozone flow rate on nanobubble generation (i) bubble size distribution (ii) scattering intensity of nanobubbles tracked at different flow rates.

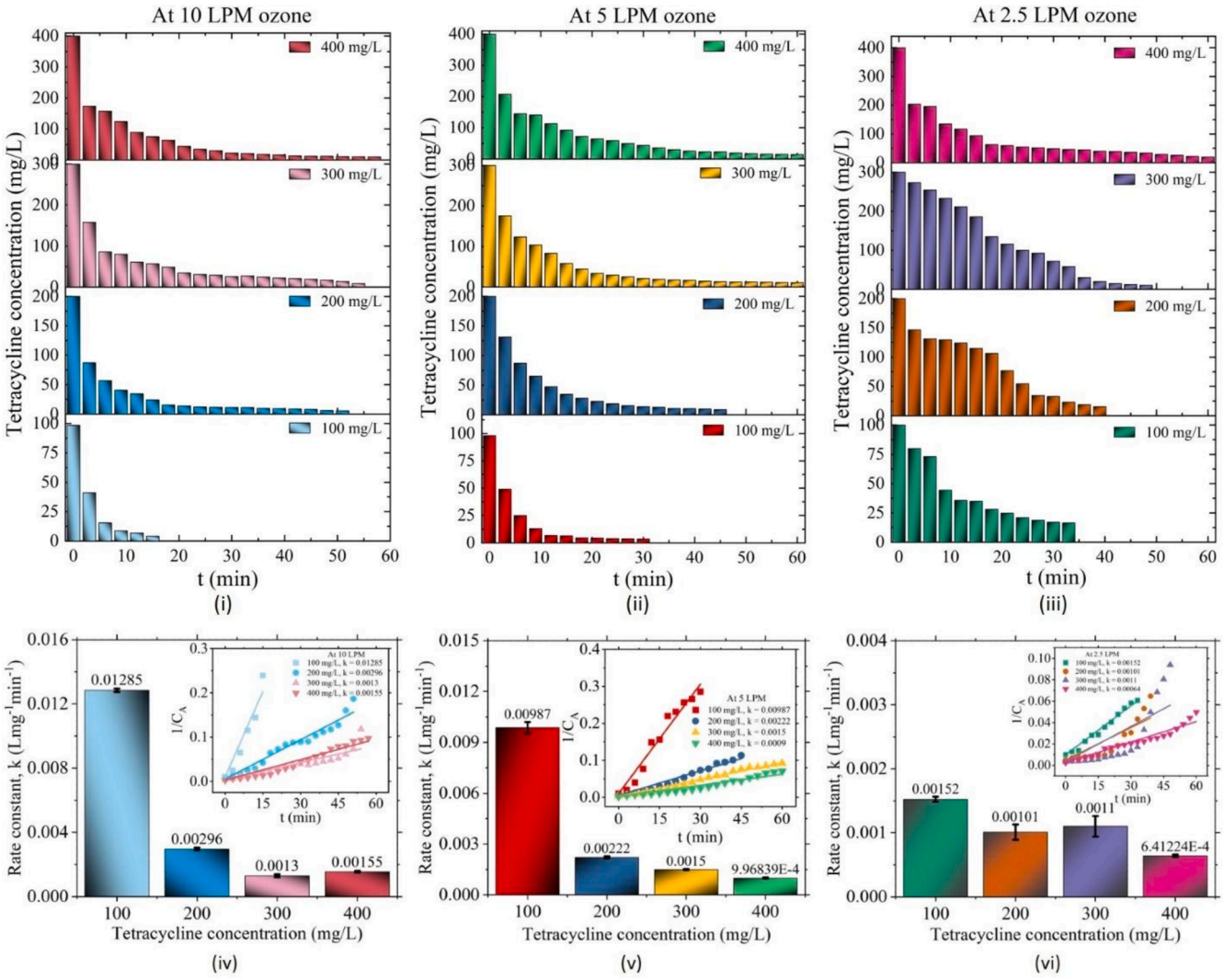

Fig. 3. Effect of Initial concentration (100–400 mg/L) and different ozone flow rates (i) 10 L/min (ii) 5 L/min (iii) 2.5 L/min and kinetics with rate constant k at (iv) 10 L/min (v) 5 L/min (vi) 2.5 L/min ozone flow rates.

the degradation. The results obtained are depicted in Fig. 4.

The results depicted in Fig. 4 were presented for a particular flow rate at 10 L/min. Fig. 4 (i) presented the amount of dissolved ozone present when no antibiotic was there compared to dissolved ozone at various concentrations of TC when degradation processes were taking place. The amount of excess ozone (mmol/L) at every point of time during the degradation process is illustrated. From Fig. 4, it can be concluded that the amount of excess ozone was being produced at each point of time. At 100 mg/L of TC concentration, since lower concentrations of contaminants were present here, a lower amount of dissolved ozone was utilised to degrade the contaminant. This can further be explained through online dissolved ozone measurements. The dissolved ozone concentration when no TC was present to various TC concentrations (100–400 mg/L) are presented in Fig. 4 (ii). From the graph, it was evident that with increase in TC concentrations, the dissolved ozone decreased as compared to the case of without TC. The difference between these concentrations would provide the amount of excess ozone present at each point as shown in Fig. 4 (i). Upon addition of TC from 100-400 mg/L, the consumption of ozone to degrade the contaminant has been depicted here where we found out that higher amount of ozone is required at higher concentrations of TC. So, out of 12 ppm of ozone concentration, 7 ppm has been consumed for the degradation of TC while the rest 5 ppm is still present as in Fig. 4 (ii). Therefore, at a low concentration of TC, the amount of excess ozone was measured to be more as compared to those at higher concentrations e.g. 400 mg/L. Also, the dissolved ozone measurements at each point of time during the degradation has been presented in Supporting Information (Fig. S2) with comparison to when no TC was present at every ozone flow rate and TC concentration. The mass transfer coefficient for each concentration of TC at different flow rates is shown in Fig. 4 (iii). The mass transfer coefficients were measured and it can be inferred that higher amount of dissolved ozone concentrations lead to increased MTC rates. At 10 L/min, 8 ppm concentration of ozone is achieved with a mass transfer coefficient of 0.32309 min-1. On the other hand, lower dissolved ozone concentrations at 2.5 and 5 L/min resulted in lower MTC values. Therefore, it can be concluded that higher the ozone flow rates, more is the dissolved ozone concentration leading to greater mass transfer rates and better degradation kinetics at the corresponding flow rates of ozone. This can be explained by the fact that higher concentrations of nanobubbles were being formed at higher flow rates. Also, increased flow rate leads to higher turbulence which creates better mixing conditions. This further helps in increasing the ozone mass transfer coefficients. The molar ratio (Ozone/TC) at each point of time was calculated and is depicted in Fig. 4 (iv). Increasing trends of molar ratio prove that excess ozone is present at each time during the degradation process. When the degradation efficiency of TC was compared to excess molar ozone as shown in Fig. 4 (iv), it could be seen that each point of degradation % corresponds to molar excess ozone %. Based on these observations, it can

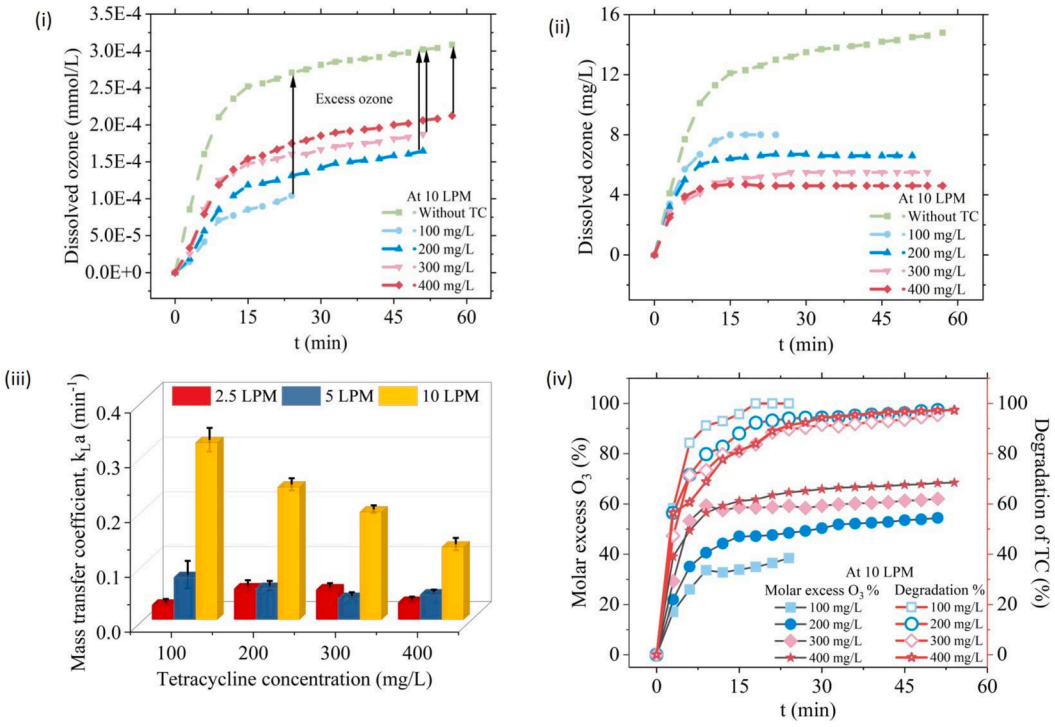

Fig. 4. (i) Dissolved ozone measurements in pure water and during tetracycline degradation (100–400 mg/L) (ii) highest dissolved ozone attained at different ozone flow rates at different TC concentrations (iii) Mass transfer coefficient corresponding to the ozone concentrations at different ozone flow rates and different concentrations of TC (100–400 mg/L) (iv) Comparison of molar excess of O_3 (%) to degradation efficiency (%) of TC (100–400 mg/L).

be concluded that molar excess of ozone serves as the limiting factor responsible for the degradation of the antibiotic. Similar trends were achieved for 2.5 and 5 L/min ozone flow rates (presented in Fig. S1, SI).

3.2. *Degradation characteristics of TC in alkaline and acidic medium*

The initial pH of the reaction mixture plays a vital role in the degradation mechanism of TC as it affects the formation of reactive radicals and the chemical activity of the ozone bubbles being formed

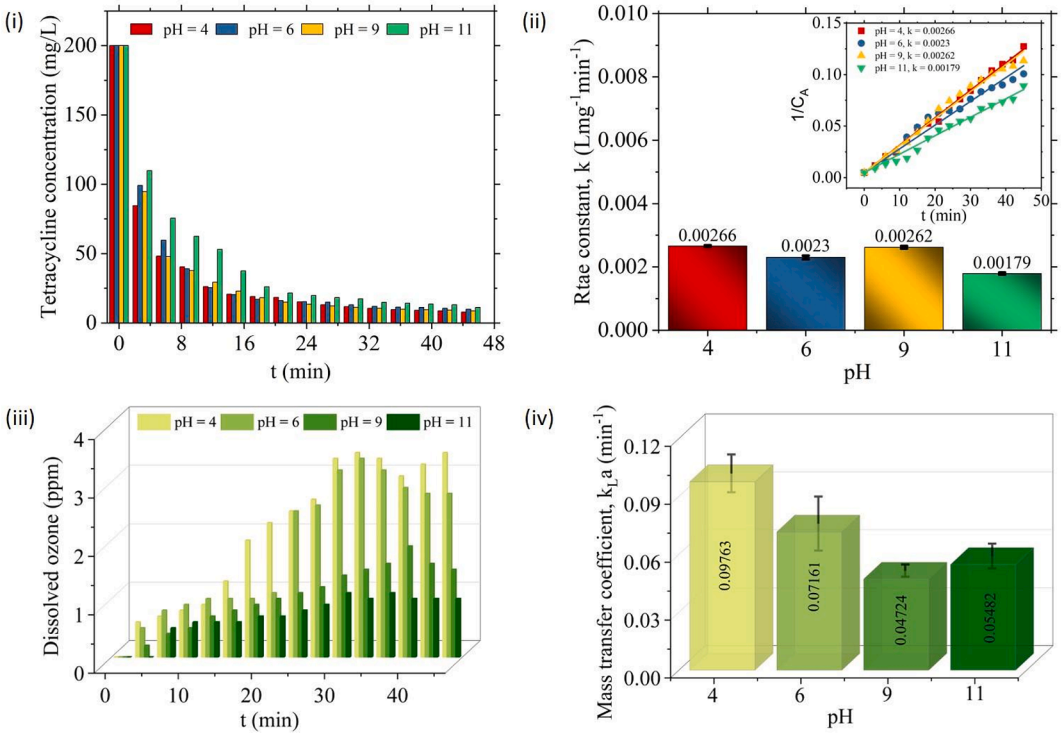

Fig. 5. Effect of acidic and alkaline mediums on degradation of TC (i) Degradation of 200 mg/L TC under different pH conditions (ii) Rate constant k under different pH conditions (iii) Online dissolved ozone measurements during degradation of TC (iv) Mass transfer coefficient of ozone at various pH conditions.

during the process [50,49]. Fig. 5 represents the experiments performed under various pH values. The effect of pH was examined by keeping TC concentration (200 mg/L) and ozone flow rates (10 L/min) constant. The pH values were varied from 4 to 11. Ozone molecules under acidic conditions may undergo the following reactions [60]:

$$O_3 \rightarrow O + O_2 \quad (8)$$

The dissociation process produces the O atom, which is thought to be the precursor for •OH in acidic ozone solutions [61].

$$O + H_2O \rightarrow 2\,HO^{\bullet} \quad (9)$$

On the other hand, ozone in the presence of OH^- (basic conditions) may be activated by the following mechanism [62]:

$$O_3 + OH^- \rightarrow O_2 + HO_2^- \quad (10)$$

$$O_3 + HO_2^- \rightarrow O_2^{\bullet -} + HO^{\bullet} + O_2 \quad (11)$$

$$O_3 + O_2^{\bullet -} \rightarrow O_3^{\bullet -} + O_2 \quad (12)$$

$$O_3^{\bullet -} + H_2O \rightarrow HO^{\bullet} + OH^- + O_2 \quad (13)$$

From Fig. 5 (i), TC degradation reached a value of 96.05 % at pH = 4, while the degradation efficiency decreased as pH was raised to 11 with 94.39 %. Acidic medium favors the degradation of TC which is consistent with literature [63,64]. The plausible reason for the efficient degradation could be the high mass transfer coefficient of ozone at low pH. Furthermore, the reaction followed pseudo-second-order kinetics as depicted in Fig. 5 (ii) with rate constant k values being highest at pH 4 (0.00266 L $mg^{-1}min^{-1}$) and lowest at pH 11 (0.00179 L $mg^{-1}min^{-1}$). The concentration of dissolved ozone increases as the pH drops. Similar trends were reported in Clever et al. [65]. When the pH dropped from 6.8 to 2.7 at 35 °C, the solubility of ozone in water increased from 6.8 ppm to 39.6 ppm. Also, Henry's law constant of ozone tends to decrease at lower pH thereby leading to a higher solubility of ozone at acidic pH [66,67]. While at basic pH, the presence of OH^- catalyses the decomposition of ozone leading to decreased dissolved ozone concentrations [68].

The pH of the solution plays a significant role as it affects the ionization of tetracycline due to its pKa values. The pKa values for TC are pKa1 (3.3), pKa2 (7.7) and pKa3 (9.5) [87]. When pH < pKa1 i.e. pH < 3.3, TC tends to exist in its protonated form (TC^+) and most TC molecules have not lost their first proton yet. When pKa1 < pH < pKa2, TC is partially ionized as it is present in both forms ((TC^+ and TC^-). At pKa2, when pH > 7.7, TC tends to exist in deprotonated form (TC^-) where most TC molecules have lost both protons. The degradation efficiencies were found to be almost similar at pH 4 and 9 with a value of 96.05 % and 95.59 % respectively within 35 min. This can be explained by the fact that dissolved ozone concentration was found to be the highest in respect to these two pH values. Further, their mass transfer coefficients were also the highest among other pH values as depicted in Fig. 5 (iv). The pH affects the activity of ozone as the mechanism of free radical generation changes with the pH. There are two mechanisms possible in which the ozone reacts at different pHs. In acidic pH, direct ozone attack is prominent while in basic mediums, ozone decomposes to form •OH radicals and ROS which further react with the organic compounds [57]. However, the degradation efficiencies at pH 4 and 9 were insignificant as after 15 min of ozonation, degradation of tetracycline reached more than 90 %, and all slightly increased to approximately 96 %. Only at pH = 11, the degradation curve is different from those of other pH values. It follows from the amount of dissolved ozone (Fig. 5(iii)). It can be elucidated that no dissolved ozone was detected during the first five minutes of the experiments, beyond which it gradually increased from 0.5 to 1.2 ppm by end of the reactions. While, for other pH values the dissolved ozone ranged from 3-4 ppm. The rate constants suggest that there was a negligible difference in the kinetics of the degradation reactions. Thus, TC was readily degraded by direct ozonation (O_3 molecule) and indirect ozonation (•OH generated by ozone and H_2O) throughout the procedure, making the difference in TC degradation at different pH levels insignificant.

3.3. Degradation kinetics in the presence of monovalent salts

To investigate the effect of the presence of salts, monovalent salts were selected for this particular study. A sodium chloride (NaCl) was used in the concentration range of 0.1–100 mM. The experimental setup was run for 30 min and the concentrations were measured within intervals of 3 min intervals. The dissolved ozone concentrations were also measured online during the experiments. A presentation of how the dissolved ozone plays a major role is depicted in Fig. S3 (in SI). From the trends, it can be stated that the ozone concentrations decrease in presence of salts as compared to that in DI water (Fig. S3 (i) SI). Also, dissolved ozone curves were compared when only salt was present to ozone concentration during degradation of TC. The graphs showed (Fig. S3 (ii) and (iii) SI) the difference in the dissolved ozone thereby claiming the amount of ozone being consumed for TC degradation. The results for the effects of salt on the degradation of TC are represented in Fig. 6. Following the observations from Fig. 6 (i), it can be exclaimed that the presence of salts or an increase in the concentration of salts declines the overall degradation of TC. The degradation of tetracycline majorly depends upon the amount of ozone being dissolved by ozone nanobubbles which has been displayed in Fig. 6 (ii). Dissolved ozone is the highest at 0.1 mM salt concentration with 1 ppm ozone concentration followed by 0.75 ppm at 10 mM salt concentration. Similarly, the mass transfer coefficients decrease with an increase in salt concentration (see Fig. 6 (iii)). The highest mass transfer coefficient values were obtained at 0.1- and 1-mM concentrations of salt and the degradation rate is highest at these two concentrations. The plausible mechanism for this can be explained by phenomenon termed as salting out effect.

The presence of salts affects the efficiency of ozone dissolution and its ability to react with the organic contaminant (TC). Higher salt concentrations reduce the contact time between ozone and TC because of the low solubility, leading to lower degradation rates and overall treatment efficiency. The dissolved ozone measured decreased with increase in salt concentrations, owing to the higher ozone decomposition rates in the presence of chloride ions. Based on the reaction kinetics, it was observed that the degradation of the TC by O_3 nanobubble follows the pseudo 2nd order reaction kinetics as shown in Fig. 6 (ii). The reaction rate constant was measured for various salt concentrations and it was almost the same with a negligible difference as depicted by the concentration profiles overlapping each other except for 100 mM salt concentration. Now, comparing the degradation efficiencies when no salts were present in the system, it can be observed that in the absence of salts the degradation was higher with 98.44 % while when the salt is added, the degradation efficiency lowers down to 94 %, thereby inhibiting the role of ozone in the presence of salts [69]. Furthermore, in the presence of salt, ozone also reacts with chloride ions, and therefore, it hinders the degradation of TC. The ozone reacts with chloride ions by following a reaction mechanism [70,71]:

$$O_3 + Cl^- \rightarrow O_2 + OCl^- \quad (14)$$

$$O_3 + OCl^- \rightarrow 2O_2 + Cl^- \quad (15)$$

These two equations (14) & (15) might be used to simulate ozone disintegration in the presence of chloride ions, which would explain the decrease in ozone lifespan and further its dissociation to superoxide radical ions. Compared to the hydroxyl radicals and ozone itself, the oxidation potential of superoxide radicals is lower. Therefore, presence of salts in the reaction systems dissociates ozone into less oxidation potential radicals thereby decreasing the overall degradation efficiency of TC.

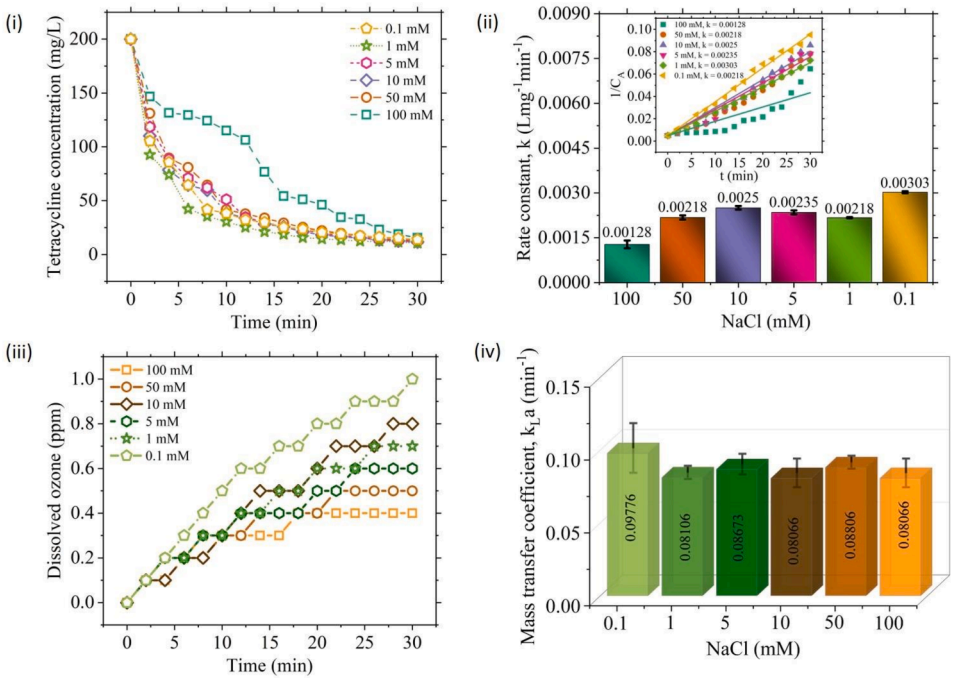

Fig. 6. Influence of monovalent salt addition on degradation of TC (i) Degradation of 200 mg/L TC under different NaCl concentrations (0.1–100 mM) (ii) Rate constant k at under different NaCl concentrations (iii) Online dissolved ozone measurements during degradation of TC (iv) Mass transfer coefficient of ozone at various salt concentrations.

3.4. Degradation efficiency of TC by different methods

To study the effect of ozone in different forms, experiments were carried out under 4 different reaction systems namely (i) O_3 NBs (ii) O_3 MBs (iii) O_2 MBs (iv) O_3 Sparging. The effect of adding H_2O_2 to each of the above reaction systems was also evaluated·H_2O_2 is considered to increase the overall oxidation potential when combined with ozone in AOPs. The first system studied the effect of O_3 NBs alone and in combination with 1 M H_2O_2. The second system consisted of O_3 MBs (prepared by MNB400 + SBT50, Riverforest Corp) alone and in the presence of 1 M H_2O_2. In the third system, the effect of oxygen MBs was measured in absence and presence of 1 M H_2O_2. The fourth system comprised of ozone being sparged directly to the stock solution through a sparger (G4 fritz quartz disc, 10 μm) in absence and presence of 1 M H_2O_2. As described in the experimental setup, the stock solutions were prepared in Milli-Q water with an initial value of tetracycline to be kept

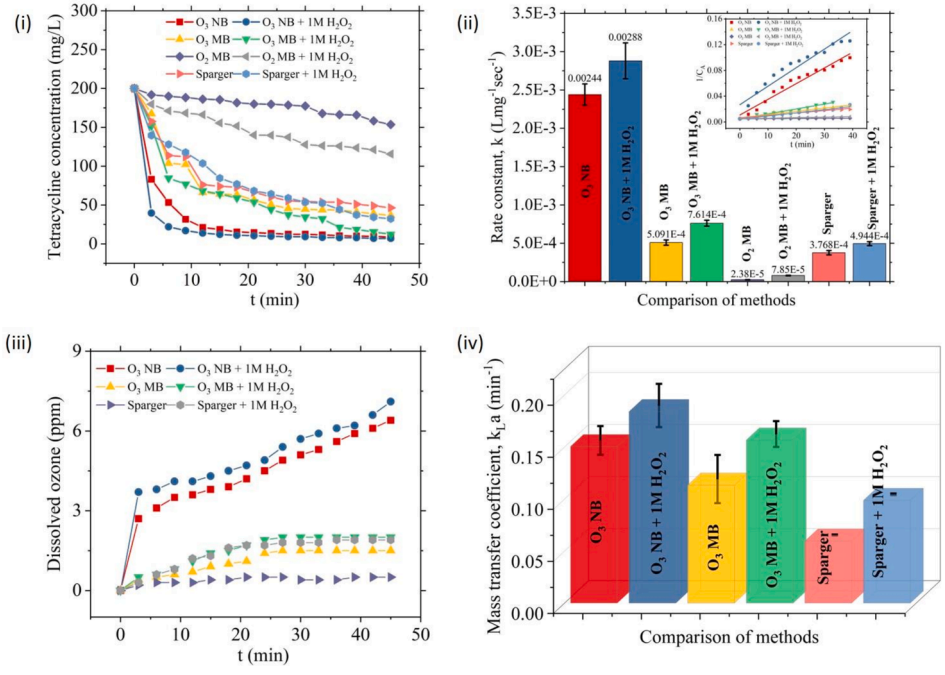

Fig. 7. (i) Comparison efficiency of different methods (ii) Pseudo second-order rate constants (iii) Dissolved ozone in ppm during each experimental condition (iv) Mass transfer coefficient for ozone at a constant concentration of Tetracycline (200 mg/L) at 10 L/min ozone and oxygen flow rates.

constant at 200 mg/L. The flow rates of oxygen and ozone were also conserved at 10 L/min. The experiments were run for 45 min and the change in concentration of TC, rate constants, and mass transfer coefficients were measured. All the results of the above-mentioned experiments are depicted in Fig. 7. The degradation curve represented in Fig. 7 (i) clearly illustrates that no significant amount of degradation of TC was observed in the case of oxygen microbubbles as compared to the ozone microbubbles through sparging. Within 45 min, 23.17 % degradation was achieved while the degradation increased to 42.17 % in case when O_2 MBs were combined with 1 M H_2O_2. Whilst in the case when ozone was being sparged to the reactor, degradation efficiency of 76.75 % was attained while adding 1 M H_2O_2 increased the degradation efficiency to 81.75 %. The effect of adding hydrogen peroxide served as a classic description of the peroxone process [72,73]. By means of electron transfer, the H_2O_2 will facilitate the O_3's breakdown; conversely, the O_3 will activate (a so-called peroxone process) the H_2O_2, producing $HO^{\bullet}$ and $HO_2^{\bullet}$ which can be shown in Eq. (15) [72]:

$$H_2O_2 + O_3 \rightarrow HO^{\bullet} + HO_2^{\bullet} + O_2 \quad (16)$$

Further, when O_3 reacts with a $HO^{\bullet}$, it can produce less reactive radicals like $HO_2^{\bullet}$, which O_3 can then transform into $^{\bullet}OH$ and O_2 as shown in Eq. (17) and (18) [74,75]:

$$HO^{\bullet} + O_3 \rightarrow O_2 + HO_2^{\bullet} \quad (17)$$

$$O_3 + HO_2^{\bullet} \rightarrow 2O_2 + HO^{\bullet} \quad (18)$$

Thus, adding H_2O_2 enhances the degradation efficiency. To study the advantage of using ozone nanobubbles, comparison of ozone nanobubbles with microbubbles was also studied. For O_3 MBs, the degradation efficiency was 83.85 % while in case of 1 M H_2O_2, it increased to 93.85 % as shown in Fig. 7 (i). Out of the four systems compared, the best degradation results were achieved for O_3 NBs as the degradation efficiency reached a maximum value of 95.73 % and 96.51 % for O_3 NBs + 1 M H_2O_2. These results can further be concluded by calculating the rate constants as shown in Fig. 7 (ii). From Fig. 7 (iii) it can be concluded that the highest concentration of dissolved ozone was produced in the presence of ozone nanobubbles + 1 M H_2O_2 with the concentration of 7.1 ppm which further decomposes and forms radicals as mentioned above due to the peroxone reactions. In case of microbubbles, the dissolved ozone 1.5 and 2 ppm in absence and presence of 1 M H_2O_2. Subsequently, when ozone was sparged in the presence or absence of 1 M H_2O_2, the concentrations reached 1.9 and 0.5 ppm, respectively. Depending upon the concentration measurements, the mass transfer coefficient was calculated for each system as depicted in Fig. 7 (iv). Clearly, the mass transfer coefficient was the highest for ozone nanobubbles + 1 M H_2O_2 (0.16401 min^{-1}), O_3 NBs alone (0.15045 min^{-1}), O_3 MBs + 1 M H_2O_2 (0.14658 min^{-1}), O_3 MBs alone (0.11335 min^{-1}) followed sparger + 1 M H_2O_2 (0.07199 min^{-1}) and lastly sparging ozone (0.00853 min^{-1}).

Furthermore, Fig. 7 (ii) shows the kinetics of the degradation of tetracycline under different conditions. The kinetic study showed that the degradation of TC exhibited a strong match with the pseudo-2nd-order reaction kinetics. The k value of TC degradation for NB + 1 M H_2O_2 (0.00288 L $mg^{-1}min^{-1}$) was 4 times higher than that of O_2 MBs + 1 M H_2O_2 (0.00007 L $mg^{-1}min^{-1}$) and 3 times higher than that of O_3 MBs + 1 M H_2O_2 (0.00076 L $mg^{-1}min^{-1}$). The findings of this study show that the incorporation of ozone nanobubbles improved the effectiveness of degradation of tetracycline (TC). This can also be validated by calculating the synergistic index (ξ) which can be determined by contrasting the rate constants of the sole processes to that of the combined processes [76]:

$$\xi = \frac{k_{combined\ process}}{\sum k_{sole\ process}} \quad (19)$$

where $\Sigma k_{sole\ process}$ will be the sum of rate constant values of individual processes and $k_{combined\ process}$ will be the sum of all the rate constants of the processes mentioned in the table. Higher values of ξ demonstrates lower influence in the degradation using O_3 in various processes. Following the above formula, the synergistic coefficient values are depicted in the Table 1.

The observed enhancement may be attributed to three variables, namely: (a) the influence of ozone in the degradation mechanism, which facilitated the generation of reactive radicals responsible for the degradation of TC (b) the stability of nanobubbles is much greater compared to regular ozone sparging. Moreover, nanobubbles exhibit a prolonged release of ozone into water, resulting in an extended duration of ozone supply. Consequently, nanobubbles provide enhanced efficiency in delivering a greater amount of ozone throughout the oxidation process (c) the increased surface area of nanobubbles has the potential to enhance mass transfer efficiency throughout the degradation process. Reactive oxygen species and radicals, such as superoxide and hydroxyl radicals [53,77], are also produced during the collapse of the nanobubble, and this might help with the TC breakdown.

In addition, to provide valuable insights on the efficiency and sustainability of using ozone nanobubbles, a quantitative comparison with the conventional AOP degradation techniques such as Fenton/Fenton like, photodegradation, photocatalysis etc. has been presented in Table 2. Parameters like degradation rates, formation of by-products, energy consumption and other operational parameters have been taken from the previous literature. These findings from the literature have been compared to the present work as in Table 2. Amongst all the AOPs listed, 100 % degradation of the antibiotic was achieved in O_3/H_2O_2/UV as well as in O3 NBs. But in case of conventional O_3, complete mineralization of antibiotic TC was not achieved. Presence of organic intermediates with high m/z values were still present even after 100 % degradation. While in case of O_3 NBs, complete degradation was achieved at varying ozone flow rates (2.5 – 10 L/min). Since 100 % degradation efficiencies were achieved at all the varying concentrations, it is an important aspect to optimize the ozone flow rates in order to provide a cost and energy efficient process. While at 10 L/min the time taken was 15 min, but for same reaction conditions 40 min were required in case of 2.5 L/min. The amount of electricity being consumed would be less when the degradation process is run for a smaller period of time. Considering the above parameters, the best operational conditions would be to run the set-up at 10 L/min in order to achieve rapid degradation and saving energy costs since very less time is required to achieve 100 % degradation.

Further, cost estimation of several oxidation processes for tetracycline degradation and their combinations have been presented in Table 3 [86]. The operational costs have been calculated for millibubble O_3, Milli bubble O_3 + Fenton, Milli bubble O_3 + Ultrasound, Millibubble O_3 + Ultrasound + Fenton with the degradation of tetracycline using ozone nanobubbles in the present work. The removal %, TC concentration and running time for each method with operation cost per run has been mentioned in Table 3 From the table, it can be clearly depicted that the cost was the lowest for ozone nanobubbles even at higher range of TC (400 mg/L) of 0.072 USD/run compared to other conventional methods.

Table 1
Synergistic index for various treatment methods in degradation of tetracycline.

Process	k ($Lmg^{-1}min^{-1}$)	ξ	$\frac{Efficiency}{Contact\ time}$(%/min)
O_3 NBs	0.00244	–	95.73/45 min
O_3 NBs + 1 M H_2O_2	0.00288	1.177	96.71/45 min
O_3 Sparger	0.000376	–	76.75/45 min
O_3 Sparger + 1 M H_2O_2	0.000494	1.294	81.75/45 min
1 M H_2O_2	0.000006	–	17.23/45 min
O_3 MBs	0.000509	–	83.85/45 min
O_3 MBs + 1 M H_2O_2	0.000761	1.478	93.85/45 min
O_2 MBs	0.0000238	–	23.17/45 min
O_3 MBs + 1 M H_2O_2	0.0000785	2.634	42.17/45 min

Table 2
Quantitative comparison of conventional AOPs to O_3 NBs for tetracycline degradation.

AOPs	Conditions	By-products	Degradation %	Energy consumption	Ref.
Fenton	H_2O_2 = 0.3 mM (Fe^{2+} = 0.003–0.3 mM) (pH = 7)	Sludge formation	76 %	Low	[93]
Fenton-like	H_2O_2 = 100 mM Fe0@CeO_2 catalyst = 0.1 g/L	Sludge formation	94 %	Low	[94]
Photo-catalysis	MIL-53 (Fe)/UV	No by-products formed	99.7 % (80 mins)	High	[95]
Photo-degradation	Mainly indirect photolysis	Biochar, syngas	89.95 %	High	[20]
O_3/H_2O_2/UV	O_3 = 0.012 mM (H_2O_2 = 0–5.9 mM) (λ = 254 nm) (pH = 8.5)	High molecular mass organics still present(Not completely mineralised)	99 %	High	[96]
O_3 NBs	6–12 mg/L dissolved ozone	No by-products formed	100 % (15 mins, 10 L/min) 100 % (25 mins, 5 L/min) 100 % (40 mins, 2.5 L/min)	High	Present work.

Table 3
Cost estimation of various AOPs for tetracycline degradation compared to O_3 NBs.

Methods	TC Removal (%)	TC Conc. (mg/L)	Running time	Operation Cost (USD/run)
Milli bubble O_3 + Fenton	98	50	10 min	0.539
Milli bubble O_3 + Ultrasound	98	50	20 min	0.655
Milli bubble O_3	98	50	20 min	0.313
Millibubble O_3 + Ultrasound + Fenton	98	50	10 min	0.371
Ozone Nanobubbles (Present study)				**(USD/run)**
1 mg/L	100	1	0.83 min	0.0013
10 mg/L	100	10	1.67 min	0.0026
50 mg/L	100	50	2 min	0.0032
100 mg/L	100	100	15 min	0.024
400 mg/L	100	400	45 min	0.072

**Here the costs were calculated based on electricity prices in Ropar, India (Rs 8 KWh^{-1}) and further converted to US $ equivalents (1 Rs. = 0.012 US $ as in July 2024).

Thus, application of ozone nanobubbles is cheaper than other conventional methods.

3.5. *Effect of radical scavengers and determining the degradation pathway*

It has been discovered that the generation of nanobubbles leads to the release of reactive oxygen species [89] which can be explained by a hypothesis termed as Rayleigh collapse [90]. It states the generation of ROS occurs through hydrodynamic cavitation such as sonication etc. where extreme pressure and temperature conditions (~10 MPa and ~5000 K) result in NB collapse. In these circumstances, it would be advantageous for water to molecularly dissociate into hydrogen atoms (·H) and hydroxyl radicals (·OH) [97]. Nevertheless, some studies showing no ROS during nanobubble generation. For instance, Chae et al. [90] found that benzoic acid degradation was not seen in the presence of oxygen nanobubbles, even when sonication was utilized to accelerate the collapse process. There was no electron paramagnetic resonance (EPR) signal. Further, it was suggested that the pressure and temperature generated by the collapse of nanobubbles would be lower than that of hydrodynamic cavitation, which might limit their capacity to facilitate the dissociation of water. However, Gaurav et al. [91] measured the formation of ROS in nanobubbles (mixture of oxygen, hydrogen and ozone) produced through electrochemical generation methods where ESR (electron spin resonance) technique was used for the analysis. It was found that the spectrum exhibits discernible peaks that bear resemblance to the presence of superoxides in the nanobubble sample. The radical quenching experiments were performed to examine the role that indirect radical oxidation ($^{\bullet}OH$, $O_2^{\bullet-}$, $^1O_2$) and direct ozone molecule oxidation play in the tetracycline's degradation. Many researchers have utilized 2-Propanol, Sodium azide, chloroform (CLF) as a scavenger of the $^{\bullet}OH$, $^1O_2$ and $O_2^{\bullet-}$ radicals respectively in oxidation experiments to comprehend the impacts of direct and indirect oxidation pathways because of the strong response it has with the radicals mentioned above [78,79,49,80]. In order to assess the total scavenging of $^{\bullet}OH$, $O_2^{\bullet-}$, $^1O_2$ radical production by ozone nanobubbles, each scavenger with a concentration of 1 mM were introduced at the start of the process. Fig. 8 (i) represents the degradation of TC in the presence and absence of radical scavengers and Fig. 8 (ii) depicts the pseudo second-order rate kinetics for the experimental runs.

It can be elucidated that in the presence of radical scavengers, the degradation efficiency decreases. The TC removal achieved a level of roughly 99 % when it was oxidized without the addition of any scavenger. Upon the addition of 1 mM 2-Propanol, the removal of TC shows a drop reaching a level of around 49.19 %, 1 mM Chloroform shows a drop to 66.37 % and 1-mM sodium azide decreases the TC efficiency to 76.75 %. This observation suggests that the degradation process of tetracycline was impeded due to the scavenging action of 2-Propanol on $^{\bullet}OH$ radicals, chloroform on $O_2^{\bullet-}$ and sodium azide on $^1O_2$. The kinetics have been displayed in Fig. 8 (ii) where the reaction rate constants have been measured and as mentioned earlier, it follows pseudo second-order kinetics. The rate constant when no scavengers were used was 0.0096 L $mg^{-1}min^{-1}$, then it decreased to 0.000410, 0.000234 and further decreased to a value of 0.000131 L $mg^{-1}min^{-1}$ at 1 mM sodium azide, CLF and 2-propanol respectively, thereby indicating the presence of radicals. Lower values of rate constant imply higher presence of that specific radical in the degradation process. Therefore, it can be concluded that $^{\bullet}OH$ radicals played predominant role followed by $O_2^{\bullet-}$ and $^1O_2$.

Given the notable improvement in the degradation efficiency of tetracycline using ozone nanobubbles, it becomes imperative to ascertain the degradation route associated with this novel synergistic activity. Consequently, a comprehensive investigation was conducted, specifically employing liquid chromatography–mass spectrometry (LC-MS). To investigate the degradation routes further, LC-MS analysis was used to identify the intermediates formed during the degradation process. The mass spectra at a time interval of 15 min are shown in Fig. S6. The mass spectra (all obtained by LC-MS technique by analysis of treated aqueous samples) of the intermediates were used for identification

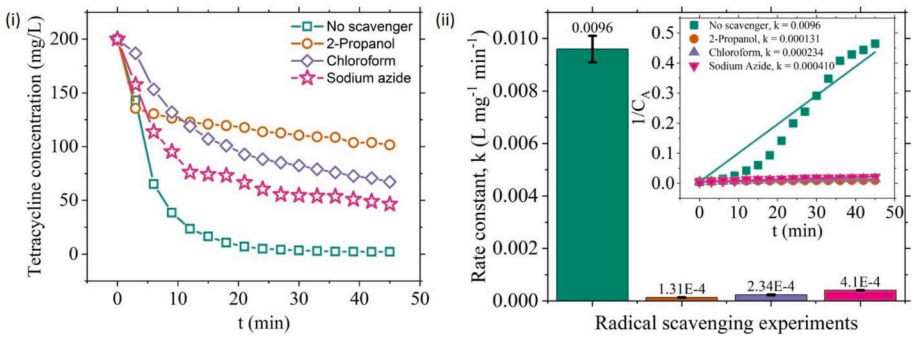

Fig. 8. Effect of addition of 2-propanol as an •OH scavenger (i) Degradation of TC (200 mg/L) under the influence of 1 mM 2-propanol, sodium azide and chloroform (ii) Pseudo second order rate constant at particular experimental conditions.

presented in Table S1 (supporting information). The proposed structure of the main intermediates has been presented along with intermediate numbers marked on degradation mechanism (Fig. 9 and Schemes 1–4). In Figure S6 at 0 min, in the first spectra, a peak of tetracycline (m/z = 445.263) was observed [58,81,82,83]. The spectra majorly displayed the intermediate products with m/z values of 445, 410, 363, 340 and 227. Notably, the degradation pathways of TC include demethylation, decarbonylation, hydrolysis, ozonolysis, decarboxylation and alcohol oxidation [84,85]. Under the constant light, active species (h+, •OH, and $O_2^{\bullet-}$) and ozone attacked the TC molecules and their intermediates, breaking them down into secondary products with a reduced molecular weight.

TC molecule (m/z = 445) when attacked by ozone (O_3 addition) during the initial stages of ozonation forms an intermediate P1 (molozonide) which is a transient and relatively an unstable compound. Further P1 rapidly decomposes to P2 (ozonide) which eventually breakdown to carbonyl compound (P3) after the oxidative step. P3 fragmented into P4 (m/z = 410) and P25 (m/z = 340). The fragmentation of P3 through oxidative demethylation, oxidation of amine, imine hydrolysis, subsequent ozonolysis and decarboxylation lead to the formation of P25 (m/z = 340) (Fig. 9). Whereas P4 may further disintegrate by 1,2,3-tricarbonyl oxidation followed by ozonation of C═C double bond at P11 to decarboxylation leading to the formation of an intermediate P15 (m/z = 362) (Fig. 9). P15 further breaks down into intermediate P18 (m/z = 226) upon decarboxylation and alcohol oxidation forming a polar intermediate (Fig. 9). Intermediates identified by LC-MS (Table S1) are marked in Fig. 9 by a frame. Since equivalent degradation products were formed when TC molecules were progressively dislodged, it was anticipated that these products would eventually disintegrate into CO_2, H_2O, NH_4^+ molecules, and other intermediates [50]. Depending upon the above degradation analysis, the chemical equation and process for the breakdown of TC by ozone nanobubbles can be presented as [62,50,87]:

$$TC + O_3 \rightarrow Products \qquad k = 0.01285\ L mg^{-1}\min^{-1} \tag{20}$$

$$O_3 + OH^- \rightarrow O_2 + HO_2^- \tag{21}$$

$$O_3 + HO_2^- \rightarrow O_2^{\bullet-} + HO^{\bullet} + O_2 \tag{22}$$

$$O_3 + O_2^{\bullet-} \rightarrow O_3^{\bullet-} + O_2 \tag{23}$$

$$O_3 + H_2O \rightarrow HO^{\bullet} + OH^- + O_2 \tag{24}$$

$$HO^{\bullet} + TC \rightarrow intermediates \rightarrow CO_2 + H_2O \tag{25}$$

$$O_2^{\bullet-} + TC \rightarrow intermediates \rightarrow CO_2 + H_2O \tag{26}$$

4. Conclusion

Tetracycline (TC) is a widely used antibiotic that is useful in treating a wide range of infectious disorders. The chemical and biological properties of tetracycline, such as its non-biodegradable nature and the development of resistance to its effects, present significant concerns. This study aimed to examine the degradation of tetracycline through ozone nanobubbles while considering various operational parameters. The results indicated that employing ozone nanobubbles at a lower pH level (pH = 4) and lower salt concentrations (0.1 mM NaCl) resulted in enhanced ozone concentration, as well as more effective degradation of tetracycline compared to other combinations. The degradation kinetics follow pseudo-second-order kinetics using ozone nanobubbles which is better compared to first-order kinetics reported for sole ozonation. It is to be noted here that comparisons were made based on the same reactor volume. After comparing the effectiveness of other methods, it was found that using ozone in the form of nanobubbles produced the best degradation efficiency. This technique could work with actual wastewater from the medical and pharmaceutical sectors since ozone nanobubbles can treat solutions with high concentrations. Preserving the high potential of ozonation requires avoiding the presence of •OH radical scavengers, such as 2-Propanol, as the oxidation process of •OH radicals are one of the essential processes in the mineralization of organic molecules. The presence of intermediates was verified through LC-MS analysis. O_3 and •OH has the ability to target the ortho or para position of the phenol ring on TC. Additional oxidation causes the unstable intermediates to ultimately breaking down into inorganic compounds like CO_2, H_2O, and NH_4^+. Ozone nanobubbles have the potential to enhance AOPs by lowering expenses and the need for chemicals. This work offers a new technique for enhancing conventional advanced oxidation processes, and nanobubbles and AOPs will play a significant role in the very effective removal of contaminants. Therefore, the best results with parameters for 100 % degradation were at 100 mg/L of TC at 8 mg/L (10 L/min) concentrations of dissolved ozone within 20 min of time span.

Future studies will focus on scaling up the ozone nanobubble technology to promote a practical approach to the degradation of wastewater containing antibiotics. Optimization of parameters such as ozone consumption, cost effectiveness, energy consumption can be studied. On the other hand, it is worth exploring the degradation mechanism of other types of antibiotics having different structural characteristics by ozone in the form of nanobubbles. Comparison of the conventional AOPs with the ozone nanobubbles in terms of degradation rates, efficiency, by-product formation and energy consumption can be carried out to get better insights on the advantages of ozone nanobubbles.

5. Environmental implication

Tetracycline in wastewater poses a serious risk to the environment and public health. AOPs such as electrocatalysis, photocatalysis etc.

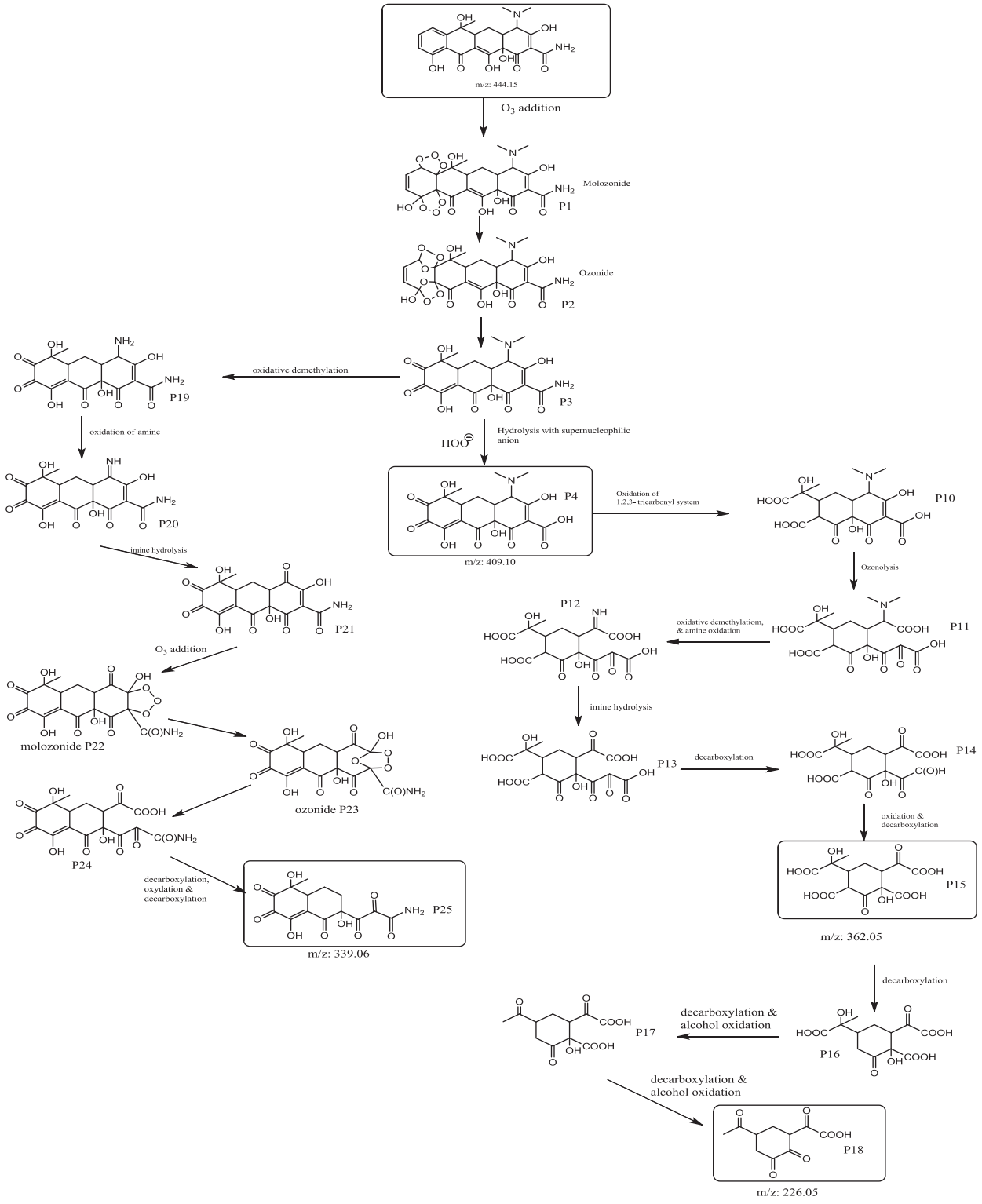

Fig. 9. Possible degradation pathway mechanism of tetracycline through LC-MS technique.

limit their commercial uses due to less stability of catalysts and prolonged operations. O_3 based AOPs are hampered by limited solubility, low mass transfer of ozone resulting in higher operation costs. This study has demonstrated a novel technique of using ozone in the form of nanobubbles as AOPs. O_3 Nanobubbles help in increasing the mass transfer coefficient thereby enhanced degradation. This work contributes to a greener and effective AOP for the degradation of antibiotics.

CRediT authorship contribution statement

Priya Koundle: Writing – original draft, Visualization, Methodology, Investigation, Formal analysis, Conceptualization. **Neelkanth Nirmalkar:** Writing – review & editing, Writing – original draft, Validation, Supervision, Resources, Project administration, Methodology, Conceptualization. **Malwina Momotko:** Writing – review & editing, Investigation, Data curation. **Sławomir Makowiec:** Writing – review &

editing, Validation, Data curation. **Grzegorz Boczkaj:** Writing – review & editing, Writing – original draft, Validation, Project administration, Methodology, Conceptualization.

Declaration of competing interest

The authors declare that they have no known competing financial interests or personal relationships that could have appeared to influence the work reported in this paper.

Data availability

No data was used for the research described in the article.

Acknowledgements

Authors would like to acknowledge Technology Innovation Hub at the Indian Institute of Technology Ropar in the framework of National Mission on Interdisciplinary Cyber-Physical Systems (NM—ICPS) for the funding of this work.

Appendix A. Supplementary data

Supplementary data to this article can be found online at https://doi.org/10.1016/j.cej.2024.156236.

References

[1] Sanjeeb Mohapatra, Sumedha Bhatia, Kavindra Yohan Kuhatheva Senaratna, Mui-Choo Jong, Chun Min Benjamin Lim, G Reuben Gangesh, Jia Xiong Lee, Goh Shin Giek, Callie Cheung, Lin Yutao, et al. Wastewater surveillance of sars-cov-2 and chemical markers in campus dormitories in an evolving covid- 19 pandemic. *J. Hazard. Mater.*, 446:130690, 2023.

[2] 2020 World Health Organization et al. Clinical management of covid-19: interim guidance, 27 may 2020. Technical report, World Health Organization, 2020.

[3] Anthony Harrington, Van Vo, Katerina Papp, Richard L Tillett, Ching-Lan Chang, Hayley Baker, Shirley Shen, Amei Amei, Cassius Lockett, Daniel Gerrity, et al. Urban monitoring of antimicrobial resistance during a covid-19 surge through wastewater surveillance. *Sci. Total Environ.*, 853:158577, 2022.

[4] Priya Nori, Kelsie Cowman, Victor Chen, Rachel Bartash, Wendy Szymczak, Theresa Madaline, Chitra Punjabi Katiyar, Ruchika Jain, Margaret Aldrich, Gregory Weston, et al. Bacterial and fungal coinfections in covid-19 patients hospitalized during the new york city pandemic surge. *Infect. Control Hospital Epidemiol.*, 42(1): 84–88, 2021.

[5] L. Cai, J. Sun, F. Yao, Y. Yuan, M.i. Zeng, Q. Zhang, Q. Xie, S. Wang, Z. Wang, X. Jiao, Antimicrobial resistance bacteria and genes detected in hospital sewage provide valuable information in predicting clinical antimicrobial resistance, Sci. Total Environ. 795 (2021) 148815.

[6] Eili Y Klein, Thomas P Van Boeckel, Elena M Martinez, Suraj Pant, Sumanth Gandra, Simon A Levin, Herman Goossens, and Ramanan Laxminarayan. Global increase and geographic convergence in antibiotic consumption between 2000 and 2015. *Proc. National Acad. Sci.*, 115(15):E3463–E3470, 2018.

[7] K. Yang, L. Li, Y. Wang, S. Xue, Y. Han, J. Liu, Airborne bacteria in a wastewater treatment plant: emission characterization, source analysis and health risk assessment, Water Res. 149 (2019) 596–606.

[8] K. Wang, S. Yang, Yu. Xin, Y. Liu, M. Bai, Xu. Yan, L. Weng, Y. Li, X. Li, Effect of microplastics on the degradation of tetracycline in a soil microbial electric field, J. Hazard. Mater. 460 (2023) 132313.

[9] G. Chu, W. Qi, W. Chen, Y. Zhang, S. Gao, Q. Wang, C. Gao, M. Gao, Metagenomic insights into the nitrogen metabolism, antioxidant pathway, and antibiotic resistance genes of activated sludge from a sequencing batch reactor under tetracycline stress, J. Hazard. Mater. 462 (2024) 132788.

[10] Zhenglu Wang, Min Cai, Peng Du, and Xiqing Li. Wastewater surveillance for antibiotics and resistance genes in a river catchment: spatiotemporal variations and the main drivers. *Water Res.*, page 121090, 2023.

[11] Christopher JL Murray, Kevin Shunji Ikuta, Fablina Sharara, Lucien Swetschinski, Gisela Robles Aguilar, Authia Gray, Chieh Han, Catherine Bisignano, Puja Rao, Eve Wool, et al. Global burden of bacterial antimicrobial resistance in 2019: a systematic analysis. *The Lancet*, 399(10325):629–655, 2022.

[12] Lu. Yu-Xiang, H. Yuan, H. Chand, Wu. You, Y.-L. Yang, H. Liang, H.-L. Song, Impacts of draw solutes on the fate of tetracycline in an osmotic membrane bioreactor: Role of the combination between membrane fouling and microorganisms, J. Hazard. Mater. 459 (2023) 132246.

[13] Akash Balakrishnan, Mahendra Chinthala, Rajesh Kumar Polagani, and Dai-Viet N Vo. Removal of tetracycline from wastewater using g-c3n4 based photocatalysts: a review. *Environ. Res.*, page 114660, 2022.

[14] Yujie Ben, Caixia Fu, Min Hu, Lei Liu, Ming Hung Wong, and Chunmiao Zheng. Human health risk assessment of antibiotic resistance associated with antibiotic residues in the environment: a review. *Environ. Res.*, 169:483–493, 2019.

[15] E. Sanganyado, W. Gwenzi, Antibiotic resistance in drinking water systems: Occurrence, removal, and human health risks, Sci. Total Environ. 669 (2019) 785–797.

[16] A. Balakrishnan, M. Chinthala, Comprehensive review on advanced reusability of g-c3n4 based photocatalysts for the removal of organic pollutants, Chemosphere 297 (2022) 134190.

[17] A. Önal, Overview on liquid chromatographic analysis of tetracycline residues in food matrices, Food Chem. 127 (1) (2011) 197–203.

[18] I. Chopra, Glycylcyclines: third-generation tetracycline antibiotics, Curr. Opin. Pharmacol. 1 (5) (2001) 464–469.

[19] G. Gopal, H. Sankar, C. Natarajan, A. Mukherjee, Tetracycline removal using green synthesized bimetallic nzvi-cu and bentonite supported green nzvi-cu nanocomposite: A comparative study, J. Environ. Manage. 254 (2020) 109812.

[20] J.J. López-Peñalver, M. Sánchez-Polo, C.V. Gómez-Pacheco, J. Rivera-Utrilla, Photodegradation of tetracyclines in aqueous solution by using uv and uv/h2o2 oxidation processes, J. Chem. Technol. Biotechnol. 85 (10) (2010) 1325–1333.

[21] I. Kim, H. Tanaka, Photodegradation characteristics of ppcps in water with uv treatment, Environ. Int. 35 (5) (2009) 793–802.

[22] J. Scaria, K.V. Anupama, P.V. Nidheesh, Tetracyclines in the environment: An overview on the occurrence, fate, toxicity, detection, removal methods, and sludge management, Sci. Total Environ. 771 (2021) 145291.

[23] R.D.C. Soltani, M. Mashayekhi, M. Naderi, G. Boczkaj, S. Jorfi, M. Safari, Sonocatalytic degradation of tetracycline antibiotic using zinc oxide nanostructures loaded on nano-cellulose from waste straw as nanosonocatalyst, Ultrason. Sonochem. 55 (2019) 117–124.

[24] Lifa Ge, Yamei Yue, Wei Wang, Fatang Tan, Shenghua Zhang, Xinyun Wang, Xueliang Qiao, and Po Keung Wong. Efficient degradation of tetracycline in wide ph range using mgncn/mgo nanocomposites as novel h2o2 activator. *Water Res.*, 198:117149, 2021.

[25] Arif Nawaz, Muhammad Atif, Adnan Khan, Mohsin Siddique, Nisar Ali, Falak Naz, Muhammad Bilal, Tak H Kim, Malwina Momotko, Hameed Ul Haq, et al. Solar light driven degradation of textile dye contaminants for wastewater treatment–studies of novel polycationic selenide photocatalyst and process optimization by response surface methodology desirability factor. *Chemosphere*, 328:138476, 2023.

[26] H. Xiong, S. Dong, J. Zhang, D. Zhou, B.E. Rittmann, Roles of an easily biodegradable co-substrate in enhancing tetracycline treatment in an intimately coupled photocatalytic-biological reactor, Water Res. 136 (2018) 75–83.

[27] W. Yang, Z. Deng, L. Liu, K. Zhou, L. Meng, L.i. Ma, Q. Wei, et al., Co-generation of hydroxyl and sulfate radicals via homogeneous and heterogeneous bi-catalysis with the eo-ps-ef tri-coupling system for efficient removal of refractory organic pollutants, Water Res. 243 (2023) 120312.

[28] A. Fernandes, P. Makoś, J.A. Khan, G. Boczkaj, Pilot scale degradation study of 16 selected volatile organic compounds by hydroxyl and sulfate radical based advanced oxidation processes, J. Clean. Prod. 208 (2019) 54–64.

[29] W.-R. Han, W.-L. Wang, T.-J. Qiao, W. Wang, Su. Hang, Xu. Chen-Xin, Wu. Qian-Yuan, Ozone micro-bubble aeration using the ceramic ultrafiltration membrane with superior oxidation performance for 2, 4-d elimination, Water Res. 237 (2023) 119952.

[30] Luyao Wang, Dan Luo, Oualid Hamdaoui, Yasser Vasseghian, Malwina Momotko, Grzegorz Boczkaj, George Z Kyzas, and Chongqing Wang. Bibliometric analysis and literature review of ultrasound-assisted degradation of organic pollutants. *Sci. Total Environ.*, 876:162551, 2023.

[31] Y. Huang, L. Li, X. Luan, X. Wei, H. Li, N. Gao, J. Yao, Ultrasound-enhanced coagulation for cyanobacterial removal: effects of ultrasound frequency and energy density on coagulation performance, leakage of intracellular organic matters and toxicity, Water Res. 201 (2021) 117348.

[32] Lu. Gonggong, X. Li, W. Li, Y. Liu, N. Wang, Z. Pan, G. Zhang, Y. Zhang, B.o. Lai, Thermo-activated periodate oxidation process for tetracycline degradation: kinetics and byproducts transformation pathways, J. Hazard. Mater. 461 (2024) 132696.

[33] Y. Shang, Xu. Xing, B. Gao, S. Wang, X. Duan, Single-atom catalysis in advanced oxidation processes for environmental remediation, Chem. Soc. Rev. 50 (8) (2021) 5281–5322.

[34] Chencheng Dong, Wenzhang Fang, Qiuying Yi, Jinlong Zhang. A comprehensive review on reactive oxygen species (ros) in advanced oxidation processes (aops). *Chemosphere*, page 136205, 2022.

[35] A. Fernandes, P. Makoś, Z. Wang, G. Boczkaj, Synergistic effect of tio2 photocatalytic advanced oxidation processes in the treatment of refinery effluents, Chem. Eng. J. 391 (2020) 123488.

[36] J. Ma, M.-H. Sui, Z.-L. Chen, L.-N. Wang, Degradation of refractory organic pollutants by catalytic ozonation—activated carbon and mn-loaded activated carbon as catalysts, Ozone Sci. Eng. 26 (1) (2004) 3–10.

[37] Rebekah Oulton, Jason P. Haase, Sara Kaalberg, Connor T. Redmond, Michael J. Nalbandian, David M. Cwiertny, Hydroxylradicalformation during ozonation of multiwalled carbon nanotubes: performance optimization and demonstration of a reactive cnt filter, Environ. Sci. Tech. 49 (6) (2015) 3687–3697.

[38] C. He, J. Wang, C. Wang, C. Zhang, P. Hou, Xu. Xieyang, Catalytic ozonation of bio-treated coking wastewater in continuous pilot-and full-scale system: Efficiency, catalyst deactivation and in-situ regeneration, Water Res. 183 (2020) 116090.

[39] C. Shan, Xu. You, M. Hua, Gu. Min, Z. Yang, P. Wang, Lu. Zhenda, W. Zhang, B. Pan, Mesoporous ce-ti-zr ternary oxide millispheres for efficient catalytic ozonation in bubble column, Chem. Eng. J. 338 (2018) 261–270.

[40] C. Li, S. Yuan, F. Jiang, Y. Xie, Y. Guo, Yu. Hang, Y. Cheng, H.e. Qian, W. Yao, Degradation of fluopyram in water under ozone enhanced microbubbles: Kinetics, degradation products, reaction mechanism, and toxicity evaluation, Chemosphere 258 (2020) 127216.
[41] G. Nam, M.M. Mohamed, J. Jung, Enhanced degradation of benzo [a] pyrene and toxicity reduction by microbubble ozonation, Environ. Technol. 42 (12) (2021) 1853–1860.
[42] Wu. Chao, P. Li, S. Xia, S. Wang, Y. Wang, Hu. Jun, Z. Liu, Yu. Shuili, The role of interface in microbubble ozonation of aromatic compounds, Chemosphere 220 (2019) 1067–1074.
[43] N. Nirmalkar, A.W. Pacek, M. Barigou, On the existence and stability of bulk nanobubbles, Langmuir 34 (37) (2018) 10964–10973.
[44] W. Fan, W. An, M. Huo, D. Xiao, T. Lyu, J. Cui, An integrated approach using ozone nanobubble and cyclodextrin inclusion complexation to enhance the removal of micropollutants, Water Res. 196 (2021) 117039.
[45] N. Nirmalkar, A.W. Pacek, M. Barigou, Interpreting the interfacial and colloidal stability of bulk nanobubbles, Soft Matter 14 (47) (2018) 9643–9656.
[46] Tao Lyu, Shubiao Wu, Robert JG Mortimer, and Gang Pan. Nanobubble technology in environmental engineering: revolutionization potential and challenges, 2019.
[47] M. Takahashi, Y. Shirai, S. Sugawa, Free-radical generation from bulk nanobubbles in aqueous electrolyte solutions: Esr spin-trap observation of microbubble-treated water, Langmuir 37 (16) (2021) 5005–5011.
[48] Mingyi Jia, Muhammad Usman Farid, Jehad A Kharraz, Nallapaneni Manoj Kumar, Shauhrat S Chopra, Am Jang, John Chew, Samir Kumar Khanal, Guanghao Chen, and Alicia Kyoungjin An. Nanobubbles in water and wastewater treatment systems: small bubbles making a big difference. *Water Res.*, page 120613, 2023.
[49] Lei Wang, Jafar Ali, Zhibin Wang, NA Oladoja, Rong Cheng, Changbo Zhang, Gilles Mailhot, and Gang Pan. Oxygen nanobubbles enhanced photodegradation of oxytetracycline under visible light: Synergistic effect and mechanism. *Chem. Eng. J.*, 388:124227, 2020.
[50] Z. Chen, Fu. Min, C. Yuan, Hu. Xueli, J. Bai, R. Pan, Lu. Peng, M. Tang, Study on the degradation of tetracycline in wastewater by micro-nano bubbles activated hydrogen peroxide, Environ. Technol. 43 (23) (2022) 3580–3590.
[51] Hu. Liming, Z. Xia, Application of ozone micro-nano-bubbles to groundwater remediation, J. Hazard. Mater. 342 (2018) 446–453.
[52] Y. Liu, H. Zhang, J. Sun, J. Liu, X. Shen, J. Zhan, A.i. Zhang, S. Ognier, S. Cavadias, P. Li, Degradation of aniline in aqueous solution using non-thermal plasma generated in microbubbles, Chem. Eng. J. 345 (2018) 679–687.
[53] P. Li, M. Takahashi, K. Chiba, Degradation of phenol by the collapse of microbubbles, Chemosphere 75 (10) (2009) 1371–1375.
[54] W. Fan, W.-G. An, Wu. Ming-xin Huo, S.-Y. Yang, S.-S. Lin, Solubilization and stabilization for prolonged reactivity of ozone using micro-nano bubbles and ozone-saturated solvent: A promising enhancement for ozonation, Sep. Purif. Technol. 238 (2020) 116484.
[55] X. Yang, L.i. Chen, S. Oshita, W. Fan, S.u. Liu, Mechanism for enhancing the ozonation process of micro-and nanobubbles: Bubble behavior and interface reaction, ACS ES&T Water 3 (12) (2023) 3835–3847.
[56] Y. Liu, B. Wang, D. Zhao, W. Jin, Xu. Feng, Y. Gao, W. Shi, H. Ren, Investigation of surfactant effect on ozone bubble motion and mass transfer characteristics, J. Environ. Chem. Eng. 11 (5) (2023) 110805.
[57] C. Wang, C.-Y. Lin, G.-Y. Liao, Degradation of antibiotic tetracycline by ultrafine-bubble ozonation process, J. Water Process Eng. 37 (2020) 101463.
[58] T. Yang, L. Zhang, F. Liu, C. Cheng, G. Li, Hydrodynamic cavitation–impinging stream for enhancing ozone mass transfer and oxidation for wastewater treatment, J. Water Process Eng. 58 (2024) 104799.
[59] H. Sharma, M. Trivedi, N. Nirmalkar, Do nanobubbles exist in pure alcohol? Langmuir (2024).
[60] K. Sehested, H. Corfitzen, J. Holcman, C.H. Fischer, E.J. Hart, The primary reaction in the decomposition of ozone in acidic aqueous solutions, Environ. Sci. Tech. 25 (9) (1991) 1589–1596.
[61] L.I.U. Limei, Z.H.A.N.G. Shuting, L.Ü. Xuebin, Y.U. Xiaoyan, Z.H.I. Suli, Ozonation of sulfur dioxide in sulphuric acid solution, Chin. J. Chem. Eng. 21 (7) (2013) 808–812.
[62] B.G. Ershov, P.A. Morozov, The kinetics of ozone decomposition in water, the influence of ph and temperature, Russ. J. Phys. Chem. A 83 (8) (2009) 1295–1299.
[63] S. Wang, X. Wang, J. Chen, Qu. Ruijuan, Z. Wang, Removal of the uv filter benzophenone-2 in aqueous solution by ozonation: kinetics, intermediates, pathways and toxicity, Ozone Sci. Eng. 40 (2) (2018) 122–132.
[64] Qu. Ruijuan, Xu. Bingzhe, L. Meng, L. Wang, Z. Wang, Ozonation of indigo enhanced by carboxylated carbon nanotubes: performance optimization, degradation products, reaction mechanism and toxicity evaluation, Water Res. 68 (2015) 316–327.
[65] H Lawrence Clever, Rubin Battino, Hiroshi Miyamoto, Yuri Yampolski, and Colin L Young. Iupac-nist solubility data series. 103. oxygen and ozone in water, aqueous solutions, and organic liquids (supplement to solubility data series volume 7). *J. Phys. Chem. Ref. Data*, 43(3), 2014.
[66] J.A. Roth, D.E. Sullivan, Solubility of ozone in water, Ind. Eng. Chem. Fundam. 20 (2) (1981) 137–140.
[67] T. Mizuno, H. Tsuno, Evaluation of solubility and the gas-liquid equilibrium coefficient of high concentration gaseous ozone to water, Ozone Sci. Eng. 32 (1) (2010) 3–15.
[68] M. Solecki, Mass Transfer: Advancement in Process Modelling, BoD–Books on Demand, 2015.
[69] A. Majumdar, U. Ghosh, A. Pal, 2d-bi4nbo8cl nanosheet for efficient photocatalytic degradation of tetracycline in synthetic and real wastewater under visible-light: Influencing factors, mechanism and degradation pathway, J. Alloy. Compd. 900 (2022) 163400.
[70] W.R. Haag, J. Hoigné, Ozonation of water containing chlorine or chloramines. reaction products and kinetics, Water Res. 17 (10) (1983) 1397–1402.
[71] M.A. Boncz, H. Bruning, W.H. Rulkens, H. Zuilhof, E.JR. Sudhölter, The effect of salts on ozone oxidation processes, Ozone Sci. Eng. 27 (4) (2005) 287–292.
[72] G. Boczkaj, A. Fernandes, P. Makos, Study of different advanced oxidation processes for wastewater treatment from petroleum bitumen production at basic ph, Ind. Eng. Chem. Res. 56 (31) (2017) 8806–8814.
[73] G. Boczkaj, A. Fernandes, Wastewater treatment by means of advanced oxidation processes at basic ph conditions: a review, Chem. Eng. J. 320 (2017) 608–633.
[74] J.J. Wu, M. Muruganandham, S.H. Chen, Degradation of dmso by ozone-based advanced oxidation processes, J. Hazard. Mater. 149 (1) (2007) 218–225.
[75] M.A. Alsheyab, A.H. Muñoz, Reducing the formation of trihalomethanes (thms) by ozone combined with hydrogen peroxide (h2o2/o3), Desalination 194 (1–3) (2006) 121–126.
[76] K. Fedorov, K. Dinesh, X. Sun, R.D.C. Soltani, Z. Wang, S. Sonawane, G. Boczkaj, Synergistic effects of hybrid advanced oxidation processes (aops) based on hydrodynamic cavitation phenomenon–a review, Chem. Eng. J. 432 (2022) 134191.
[77] P. Li, M. Takahashi, K. Chiba, Enhanced free-radical generation by shrinking microbubbles using a copper catalyst, Chemosphere 77 (8) (2009) 1157–1160.
[78] Erika Reisz, Clemens von Sonntag, Agnes Tekle-Röttering, Sergej Naumov, Winfried Schmidt, and Torsten C Schmidt. Reaction of 2-propanol with ozone in aqueous media. *Water Res.*,, 128:171–182, 2018.
[79] J.J. Wu, J.S. Yang, M. Muruganandham, C.C. Wu, The oxidation study of 2-propanol using ozone-based advanced oxidation processes, Sep. Purif. Technol. 62 (1) (2008) 39–46.
[80] K. Fedorov, M.P. Rayaroth, N.S. Shah, G. Boczkaj, Activated sodium percarbonate-ozone (spc/o3) hybrid hydrodynamic cavitation system for advanced oxidation processes (aops) of 1, 4-dioxane in water, Chem. Eng. J. 456 (2023) 141027.
[81] Min Fu, Chenxi Yuan, Jinwu Bai, and Youzhou He. Degradation of tetracycline in wastewater by persulfate activated with micro-nano bubbles. *Available at SSRN 4055015*.
[82] G. Yang, Y. Liang, Z. Xiong, J. Yang, K. Wang, Z. Zeng, Molten salt-assisted synthesis of ce4o7/bi4moo9 heterojunction photocatalysts for photo-fenton degradation of tetracycline: Enhanced mechanism, degradation pathway and products toxicity assessment, Chem. Eng. J. 425 (2021) 130689.
[83] C. Lai, Z. An, H. Yi, X. Huo, L. Qin, X. Liu, B. Li, M. Zhang, S. Liu, L. Li, et al., Enhanced visiblelight-driven photocatalytic activity of bismuth oxide via the decoration of titanium carbide quantum dots, J. Colloid Interface Sci. 600 (2021) 161–173.
[84] M. Wang, S. Li, J. Kang, Y. Tang, J. Wang, Xu. Zhenqi, J. Liu, Enhanced tetracycline degradation by nc codoped fe2o3 with rich oxygen vacancies in peroxymonosulfate assisting photoelectrochemical oxidation system: performance, mechanism and degradation pathway, Chem. Eng. J. 451 (2023) 138611.
[85] Y. Bi, L. Huang, X. Song, T. Sun, Xu. Shimin, Fe-based prb system with ultrasound synergistically enhances the degradation of tetracycline, Chem. Eng. Process.-Process Intensif. 197 (2024) 109687.
[86] C. Wang, C.-Y. Lin, G.-Y. Liao, Feasibility study of tetracycline removal by ozonation equipped with an ultrafine-bubble compressor, Water 13 (8) (2021) 1058.
[87] Zachary R Hopkins, Lee Blaney. A novel approach to modeling the reaction kinetics of tetracycline antibiotics with aqueous ozone. Sci. Total Environ., 468:337-344,2014.
[88] M. Hammad Khan, H. Bae, J.-Y. Jung, Tetracycline degradation by ozonation in the aqueous phase: proposed degradation intermediates and pathway, J. Hazard. Mater. 181 (1–3) (2010) 659–665.
[89] A. Agarwal, W.J. Ng, Yu. Liu, Principle and applications of microbubble and nanobubble technology for water treatment, Chemosphere 84 (9) (2011) 1175–1180.
[90] S.H. Chae, M.S. Kim, J.-H. Kim, J.D. Fortner, Nanobubble reactivity: evaluating hydroxyl radical generation (or lack thereof) under ambient conditions, ACS Es&t Eng. 3 (10) (2023) 1504–1510.
[91] G. Yadav, N. Nirmalkar, C.-D. Ohl, Electrochemically reactive colloidal nanobubbles by water splitting, J. Colloid Interface Sci. 663 (2024) 518–531.
[92] P. Seridou, N. Kalogerakis, Disinfection applications of ozone micro-and nanobubbles, Environ. Sci. Nano 8 (12) (2021) 3493–3510.
[93] Rama Pulicharla, Satinder Kaur Brar, Tarek Rouissi, Serge Auger, Patrick Drogui, Mausam Verma, and Rao Y Surampalli. Degradation of chlortetracycline in wastewater sludge by ultrasonication, fenton oxidation, and ferro-sonication. Ultrasonics Sonochem., 34:332–342,2017.
[94] N. Zhang, J. Chen, Z. Fang, E.P. Tsang, Ceria accelerated nanoscale zerovalent iron assisted heterogenous fenton oxidation of tetracycline, Chem. Eng. J. 369 (2019) 588–599.
[95] Y. Zhang, J. Zhou, J. Chen, X. Feng, W. Cai, Rapid degradation of tetracycline hydrochloride by heterogeneous photocatalysis coupling persulfate oxidation with mil-53 (fe) under visible light irradiation, J. Hazard. Mater. 392 (2020) 122315.
[96] H. Lee, E. Lee, C.-H. Lee, K. Lee, Degradation of chlorotetracycline and bacterial disinfection in livestock wastewater by ozone-based advanced oxidation, J. Ind. Eng. Chem. 17 (3) (2011) 468–473.
[97] K. Yasui, On some aspects of nanobubble-containing systems, Nanomaterials 12 (13) (2022) 2175.